

REAL-TIME CORROSION MONITORING IN A PROCESS STREAM OF A CHEMICAL PLANT USING COUPLED MULTIELECTRODE ARRAY SENSORS

Lietai Yang and Narasi Sridhar
Southwest Research Institute
6220 Culebra Road
San Antonio, TX 78238 USA

Steven L. Grise, Brian J. Saldanha, Michael H. Dorsey,
Heather J. Shore and Amanda L. Smith
DuPont, Wilmington, DE 19898

ABSTRACT

Coupled multielectrode array sensors made of Type 316L stainless steel, AL6XN and Alloy C-276 alloys were used as real time-sensors to monitor localized corrosion in a side loop of a process stream in a chemical plant. The pitting corrosion rates measured from the probes made of stainless steel and nickel-chromium alloys are consistent with the pitting resistance equivalent numbers of the alloys and with the plant experience. The pitting rate obtained from the long-term measurement is in good agreement with the actual corrosion rate obtained from the posttest surface examination of the probes.

Keywords: Corrosion monitoring, pitting corrosion, localized corrosion, stainless steel, nickel-base alloys, corrosion sensor, multielectrode array sensor

INTRODUCTION

As part of the effort to develop a general model for predicting the occurrence of localized corrosion in chemical process streams¹, real-time monitoring tests were conducted in a plant process stream using coupled multielectrode array sensors to validate the model.

The monitored process stream consisted of a nearly-saturated chloride brine. Minor impurities included iron (Fe), copper (Cu), nickel (Ni) and magnesium (Mg). None of the impurities exceeded a concentration of 10 mg/L. Nominal operating conditions involved a temperature of 100°C, pH ranging from 8 to 10, and liquid superficial velocity of 2 ft/sec (0.61 m/sec) through the loop. Results reported in this paper are from the plant monitoring tests.

EXPERIMENTAL

Coupled Multielectrode Array Sensors

The principle of the coupled multielectrode array sensor (MAS) has been described elsewhere.² In a MAS, multiple miniature electrodes are the active sensing element of the sensor. These miniature electrodes are made of metals identical to the material of construction of the process, and whose corrosion rate is of monitoring interest and are coupled to a common joint through independent resistors. Thus, each electrode simulates or represents part of a corroding metal if the sensor is in a corrosive environment. In a localized corrosion environment, anodic currents flow into the more corroding electrode and cathodic currents flow out of the less or non-corroding electrodes. Such currents are measured from the voltages across the resistors and are used as the signals for localized corrosion.

This technology has been tested extensively for carbon steels, stainless steels, and nickel-based alloys in cooling water, under salt- or bio-deposits, and concentrated chloride solutions³. Three MAS probes were used, each consisting of eight identical solution annealed wires of stainless steel 316L (UNS S31603), AL6XN (UNS N08367) and Alloy C-276 (UNS N10276). The compositions of these alloys are shown in Table 1 and the probes are shown in Figure 1. The probes were designed for applications at pressures as high as 1600 psi (10.88 MPa) and temperatures as high as 230 °C. The tubing material for all the probes was Alloy C-276. The sensing electrodes were flush mounted in Polytetrafluoroethylene (PTFE). The surface area of each electrode in the sensors was 0.00567 cm². Prior to the test, the sensing surfaces of the probes were polished with 600-grit paper and cleaned with acetone.

Test Loop in the Process Stream

A side loop was constructed out of Alloy C-22 (UNS N06022) into which the MAS probes, Linear Polarization Resistance (LPR) probes, and a high-temperature reference electrode were installed.¹ The reference electrode was an external pressure-balanced Ag/AgCl electrode⁴. The LPR probes were for a different test and their results are not reported in this paper. Figure 2 shows the arrangement of the probes in the pressurized test loop. Data for the MAS probes and electrochemical potentials were collected via a fiber-optic cable in the plant digital control system and downloaded remotely.

RESULTS AND DISCUSSIONS

Short-term Monitoring

Figure 3 shows the localized corrosion signals (current densities) for the different probes obtained during the initial periods after emplacement. Figure 4 shows the apparent pitting rate obtained by dividing the localized corrosion current signal by the apparent surface area of the electrode². The apparent surface area is the total area exposed to the electrolyte, including the sections that were not corroded. The apparent pitting rate from the Type 316L stainless steel was significantly higher than those from the AL6XN and Alloy C-276 alloys. The apparent pitting rate from the Alloy C-276 probe was the lowest and, in three days, it decreased to 3 μm /year (0.11 mil/year), which is close to the background noise or the lower detection limit of the system under the test conditions (0.45 μm/year or 0.018 mil/year). The variation in the apparent pitting rates from the three probes was more than 3 orders of magnitude.

Figure 5 shows the potentials of the sensors (measured at the joint where all the electrodes were coupled together for each sensor²) and the piping of the side loop. The potentials of Alloy C-276 and AL6XN were significantly more noble than those of the Type 316L stainless steel, indicating that the Type 316L stainless steel was undergoing active corrosion while Alloy C-276 and AL6XN were experiencing passive behavior. In addition, the corrosion potential of the Alloy C-276 probe was, in most cases, higher than that of AL6XN. Therefore, the results in Figure 5 are consistent with those in Figures 3 and 4.

The potential of the piping of the side loop was low and very close to that of the Type 316L stainless steel probes (Figure 5). This was surprising as the side loop is constructed of Alloy C-22, and its potential would have been expected to be closer to that of Alloy C-276. In addition, inspections of this piping did not indicate any active or localized corrosion. Therefore, the much lower corrosion potential of the piping suggests that there must be some other components of the piping system must be undergoing active corrosion. Apparently, the active material was not the loop itself. As the solution contained a high concentration of salts and was highly conductive, the low corrosion potential may have been a reflection of other more active components even though they might be some distance away from the side loop.

The following formulae have been suggested for calculating the pitting resistance equivalent numbers (PREN) according to the alloy compositions.^{5,6}

$$\text{PREN} = \% \text{Cr} + 3.3\% \text{Mo} + 20\% \text{N} \quad (1)$$

for stainless steels, and

$$\text{PREN}' = \% \text{Cr} + 3.3\% (\text{Mo} + \text{W}) + 30\% \text{N} \quad (2)$$

for nickel based alloys. In Equations (1) and (2), the elemental compositions are in weight or atomic percents.

Table 2 presents the values of the calculated PREN or PREN' by weight and by atomic compositions. The relative results as shown in Figures 3, 4 and 5 are in quantitative agreement with the pitting resistance equivalent numbers: 316SS < AL6XN < Alloy C-276.

The results for 316L stainless steel, AL6XN and Alloy C-276 alloys as shown in Figure 4 also agree with the plant experience. Failures have been observed with the Type 316L stainless steel components in the same process stream in the past, and these components have been replaced with more corrosion-resistant alloy metallurgy, such as Alloy C-276, which has performed well in the system for years.

Long-Term Monitoring

The apparent pitting rates for three different probes obtained in a 45-day monitoring period are presented in Figure 6. After a few weeks of exposure, the apparent pitting rates from all the probes decreased significantly. There were also significant fluctuations in the measured apparent pitting rates. Many of the fluctuations coincided with the short-term shutdown and start-up of the side loop. These shutdown and start-up activities inevitably caused sudden changes in fluid flow dynamics and temperature. The temperature usually dropped to ambient when the side loop was shutdown because it was not heated or insulated. Figure 6 also shows that localized corrosion continued even when the system was shutdown because the process fluid was still in contact with the probes.

At the end of the 45-day exposure, the probes were retrieved from the plant and examined. A dense and uniformly distributed layer of scale covered most surfaces exposed to the system fluid, including the sensing electrodes (Figure 7). There were also small areas where the scale had spalled off. The scale was identified as carbonate using Raman Spectroscopy; it was hard and could not easily be removed from the substrate with a soft brush. Therefore, the decrease in pitting rates as shown in Figure 6 after a few weeks of exposure is suspected to be due to the formation of the scale, as it would hinder mass transport at the electrode surface and thus reduce the pitting rate. On the other hand, if a spalling event took place on one or more electrodes, the pitting rate for the probe would revert to a higher value. Such a spalling event may be triggered by sudden changes in fluid flow or temperature. This is probably why many of the sudden increases in pitting rate for the Type 316 stainless steel probe as shown in Figure 6 overlapped with the start-up events.

Figure 8 shows the electrochemical potentials of the three probes and the system piping during the long-term measurement. The potentials from all the probes increased over time. However, the potential of the piping remained essentially the same. A similar influence of shutdown/start-up activities on corrosion is

represented by the shifts in the corrosion potential toward a more noble state after restart of the process. This is consistent with the apparent pitting rates shown in Figure 6.

Figure 9 shows a typical comparison between the apparent pitting rate and the potential from the Type 316L stainless steel probe. Increases in potential generally overlap with the decreases in the apparent pitting rates or the decreases in corrosion activity.

The electrode surfaces of the different probes were examined using an optical microscope after being cleaned with a hard brush. Some of the electrodes of the Type 316L stainless steel sensor were indeed severely corroded (Figure 10). In Figure 10, about 40% of the sensing surface of the most corroded electrode (electrode E6) were severely pitted and the other 60% were relatively intact. The maximum depth of the pit was found to be about 0.25 mm, which corresponds to an average rate of 2.0 mm/y. The measured average apparent pitting rate for the Type 316L stainless steel probe as shown in Figure 6 is 1.04 mm/year. After accounting for the non-uniform surface factor² (dividing the apparent rate by 0.4 or replacing the apparent surface area with the truly corroded surface area in the calculation of the pitting rate), the modified average pitting rate from the probe during the 45-day monitoring period is 2.6 mm/year, which is close to the actual rate measured after the test (2.0 mm/y).

The surfaces of the AL6XN and the Alloy C-276 probes did not show significant corrosion under the microscope (Figures 11 and 12). This is consistent with the results in Figure 6, because the calculated apparent cumulative depths for the two probes are less than 3 μm , which is beyond the resolution of the microscope.

The long-term measurement results were affected by the formation of the scales. However, if the probes are installed in a proper location, it may give the real corrosion rate for system components of interest because the corrosion rate of the system components is also affected by the formation of scale. If the probe cannot be installed where conditions, including the flow dynamics and temperature, are representative of those experienced by system components, the rate measured with the freshly polished probe may be used as a conservative estimate.

CONCLUSIONS

Real-time measurements of localized corrosion rate were conducted in a pressurized side loop of a process stream in a chemical plant for three types of alloys, Type 316L stainless steel, AL6XN and Alloy C-276. The measured order of resistance to localized corrosion for the different alloys in the system is 316L SS < AL6XN < Alloy C-276. This order is consistent with the plant experience and the pitting resistance equivalent numbers of the alloys.

There was also good correlation between the apparent current density of the 316L versus actual measured depth of attack. The measured average pitting rate for the Type 316L stainless steel is about 2.6 mm/year, which is close to the value obtained from the posttest examination on the probe.

Long-term measurements of the localized corrosion for the different alloys showed that the corrosion rates for the different alloys decreased significantly after a few weeks of exposure. The decrease was attributed to the formation of a hard layer of scale on the sensing surface. The hard layer of scale was identified as carbonate using Raman Spectroscopy.

ACKNOWLEDGMENTS

The work reported in this paper is being funded by the National Institute of Standards and Technology Advanced Technology Program. The authors acknowledge the assistance of Bryan Derby (Southwest Research Institute) in assembling some of the probe components used in the plant and the technical discussions with Andre Anderko (OLI Systems). The authors thank the Southwest Research Institute Advisory Committee for Research (SwRI-ACR) for its support of the development of the MAS probe and Haynes International for providing the materials for constructing the test loop used in the plant.

REFERENCES

1. Anderko, A., N. Sridhar, C.S. Brossia, D.S. Dunn, L.T. Yang, B.J. Saldanha, S.L. Grise, and M.H. Dorsey. "An Electrochemical Approach to Predicting and Monitoring Localized Corrosion in Chemical Process Streams." Proceedings of the CORROSION 2003 Conference. Paper No. 03375. Houston, Texas: NACE International. 2003.
2. Yang, L., N. Sridhar, O. Pensado, and D.S. Dunn. "An *In-Situ* Galvanically Coupled Multielectrode Array Sensor for Localized Corrosion." *Corrosion*. Vol. 58, No. 1004. 2002.
3. Yang, L. and N. Sridhar. "Coupled Multielectrode Online Corrosion Sensor." *Materials Performance*. p. 48. September 2003.
4. Macdonald, D.D., A.C. Scott, and P. Wentreek. "External Reference Electrodes for High Temperature and High Pressure Aqueous Systems." *J. Electrochem. Soc.* Vol. 126, No. 908. 1979.
5. Sedricks, A.J. "Effect of Alloy Composition and Microstructure on the Passivity of Stainless Steels." *Corrosion*. Vol. 42. p. 376. 1986.
6. Rebak, R.B. and P. Crook. "Improved Pitting and Crevice Corrosion Resistance of Nickel and Cobalt Based Alloys." Proceedings of the Symposium on Critical Factors in Localized Corrosion III. R.G. Kelly, G.S. Frankel, P.M. Natishan and R.C. Newman, eds. Pennington, New Jersey: Electrochemical Society. pp. 289–302. 1999.

TABLE 1.
CHEMICAL COMPOSITIONS (WT %) OF THE ALLOYS USED IN THE SENSORS

Alloys	UNS #	Fe	Ni	Cr	Mo	Cu	W	C	Others
316L SS	S31603	Bal.	12	17.58	2.1	0.31		0.028	Mn=1.4
AL6XN	N08367	48.22.	23.92	20.43	6.19	0.16	0.03	0.02	—
C-276	N10276	5.51	58.75	15.64	15.54	0.19	3.74	0.002	Mn=0.41 Co=0.17

TABLE 2
PITTING RESISTANCE EQUIVALENT NUMBERS FOR THE ALLOYS TESTED

Basis	Formula ^{5,6}	316L SS	AL6XN	C-276
Mass Composition	%Cr+3.3%Mo+20%N, for SS	24.5	—	—
	%Cr+3.3%(Mo+W)+30%N, for Ni Based Alloy	24.5	41.0	79.3
Atomic Composition	%Cr+3.3%Mo+20%N, for SS	22.9	—	—
	%Cr+3.3%(Mo+W)+30%N, for Ni Based Alloy	22.9	35.1	56.8



FIGURE 1. Coupled multi-electrode array sensor (MAS) probes for application in a pressurized process stream at elevated temperatures



FIGURE 2. Three MAS probes (two on the right flange and one at bottom of left flange) and an external pressure-balanced Ag/AgCl reference probe (at top of left flange) in the side loop of a process stream in a chemical plant. Also shown are standard linear polarization resistance (LPR) probes on the middle flange.

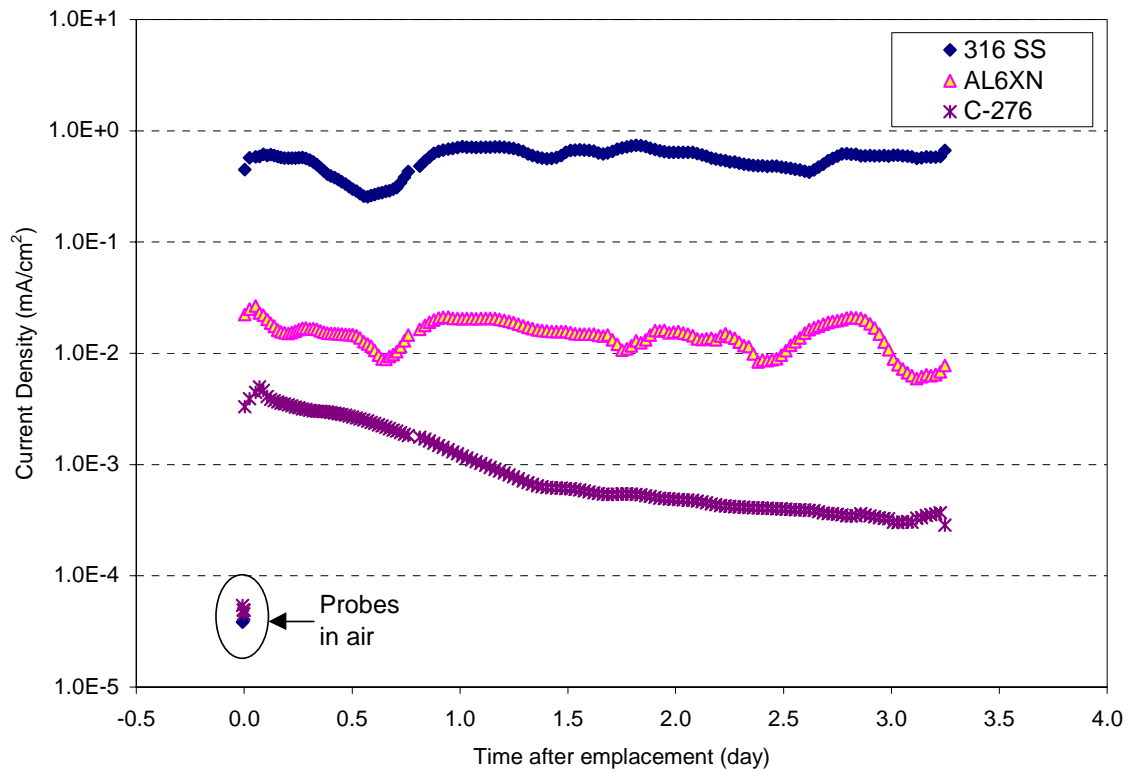


FIGURE 3. Localized corrosion signals from the different probes in a side loop of a pressurized process stream during the initial monitoring periods. At time zero, the probes were exposed to flowing process fluid. The signals measured in air correspond to the background noise, and/or the lower detection limit of the system under the test conditions.

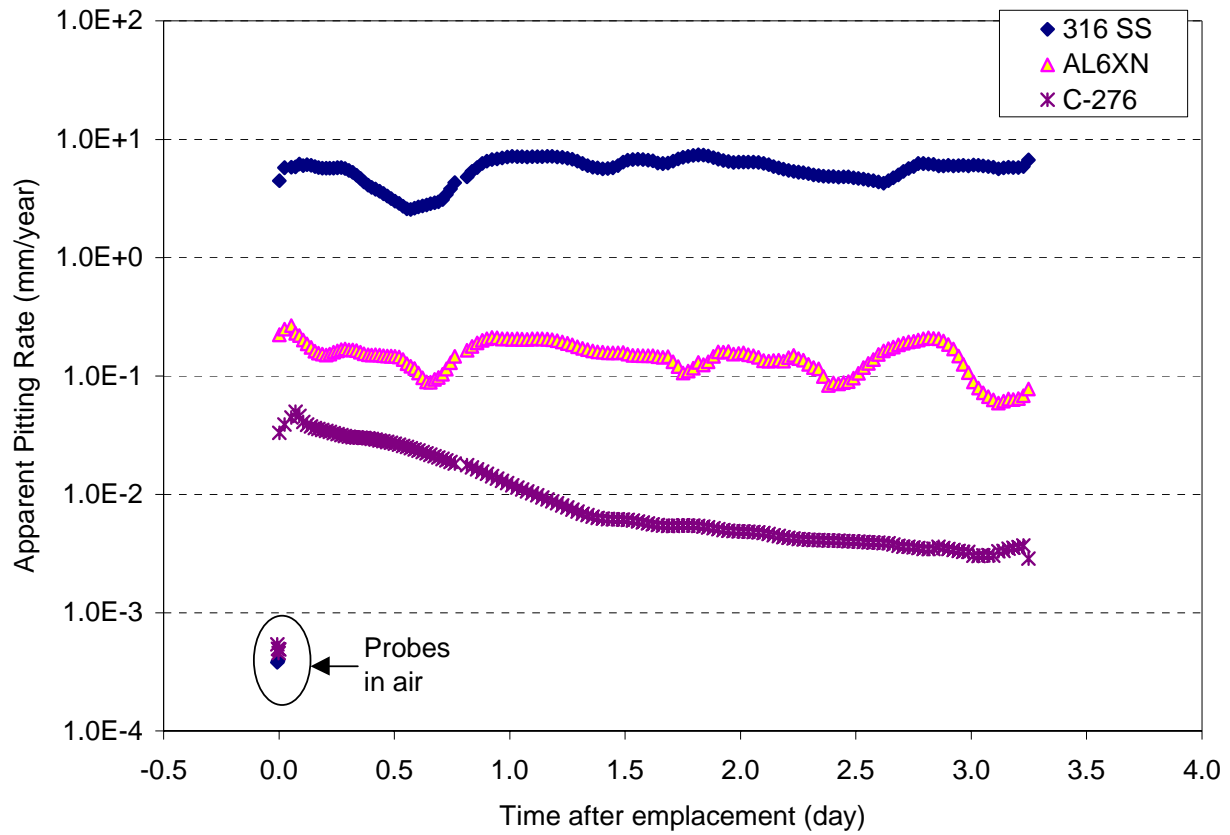


FIGURE 4. Apparent pitting rate from the different probes in a side loop of a pressurized process stream during the initial monitoring periods as indicated in Figure 3.

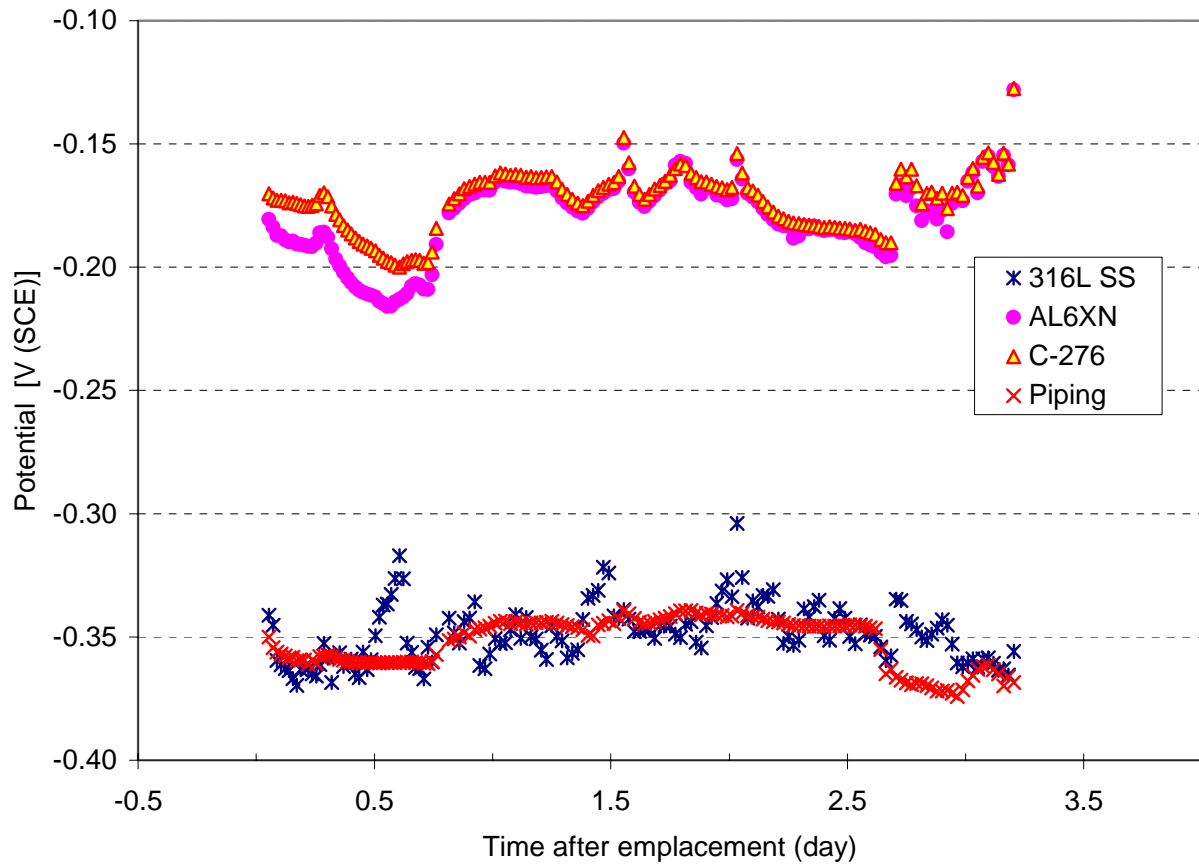


FIGURE 5. Electrochemical potentials of the different probes and the piping of the side loop during the time as shown in Figures 3 and 4.

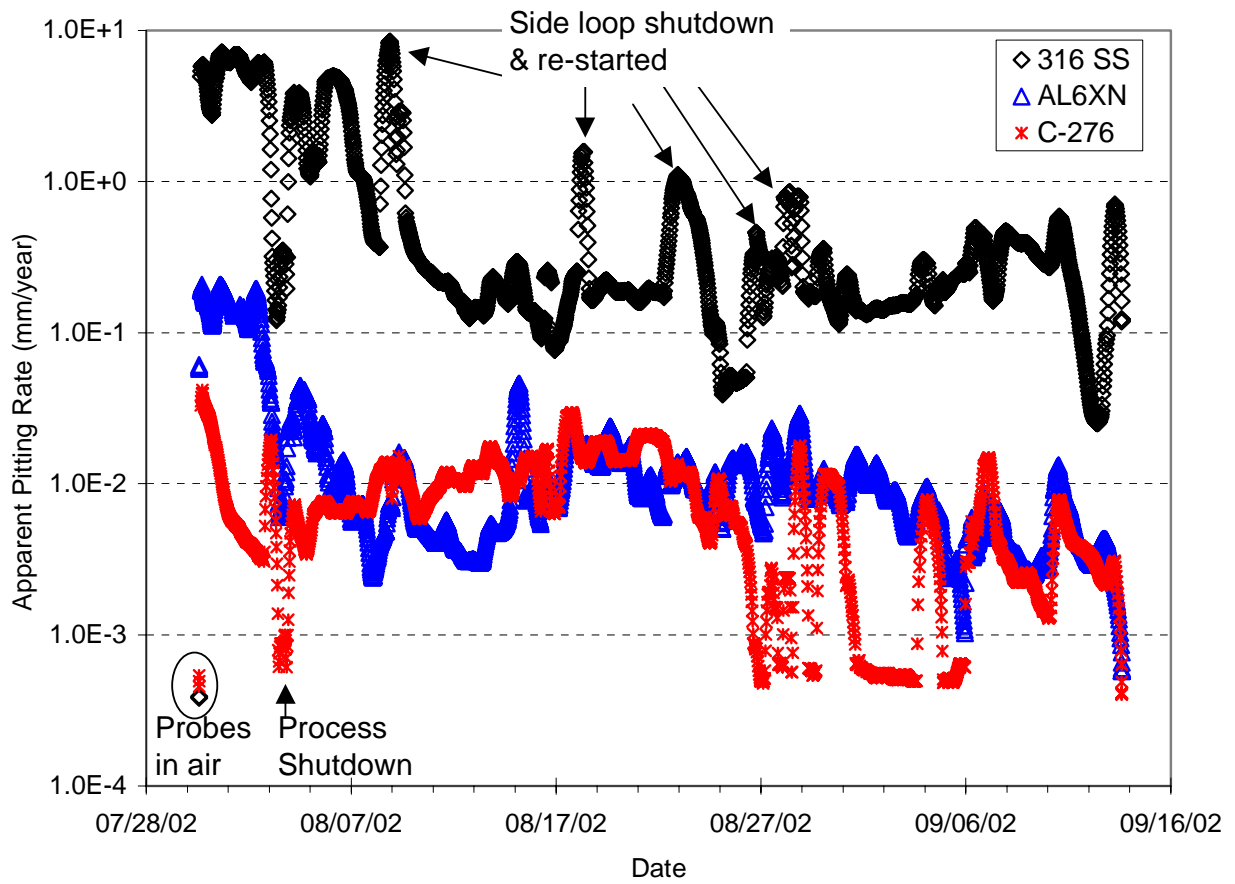


FIGURE 6. Apparent pitting rates from different probes in a side loop of a hot brine process stream during a 45-day monitoring period. Many of the corrosion-rate peaks coincide with the side loop shutdown and start-up, which involved changes in both fluid flow and temperature.

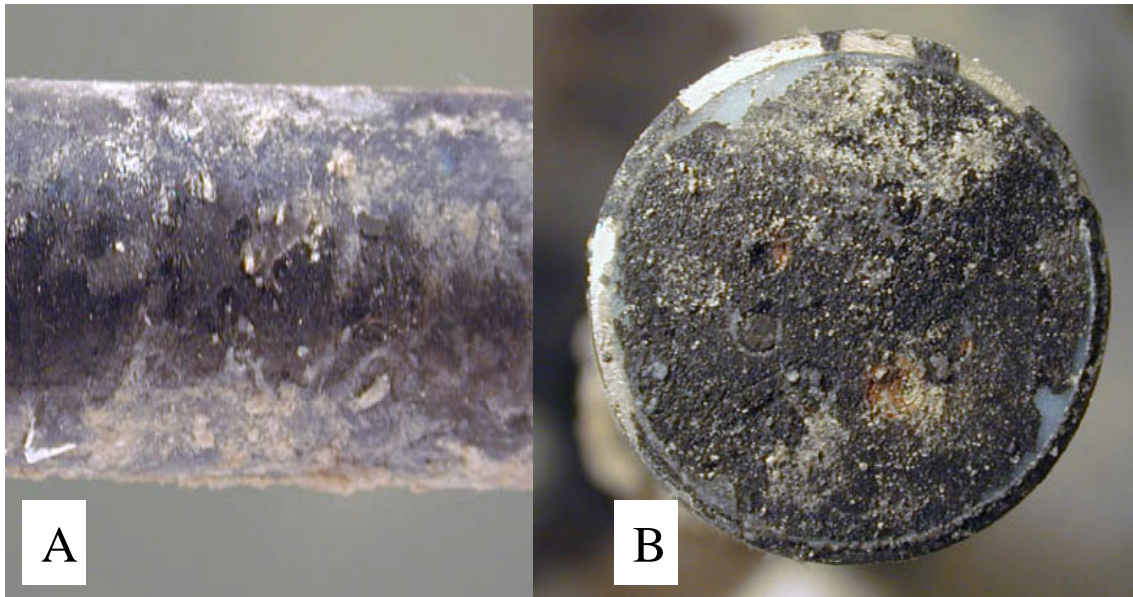


FIGURE 7. Hard and dense scales were typically formed on the side (A) and sensing surface (B) of the monitoring probes after 45-day service in the side loop of a hot brine stream. The black scales were identified as carbonates using Raman Spectroscopy.

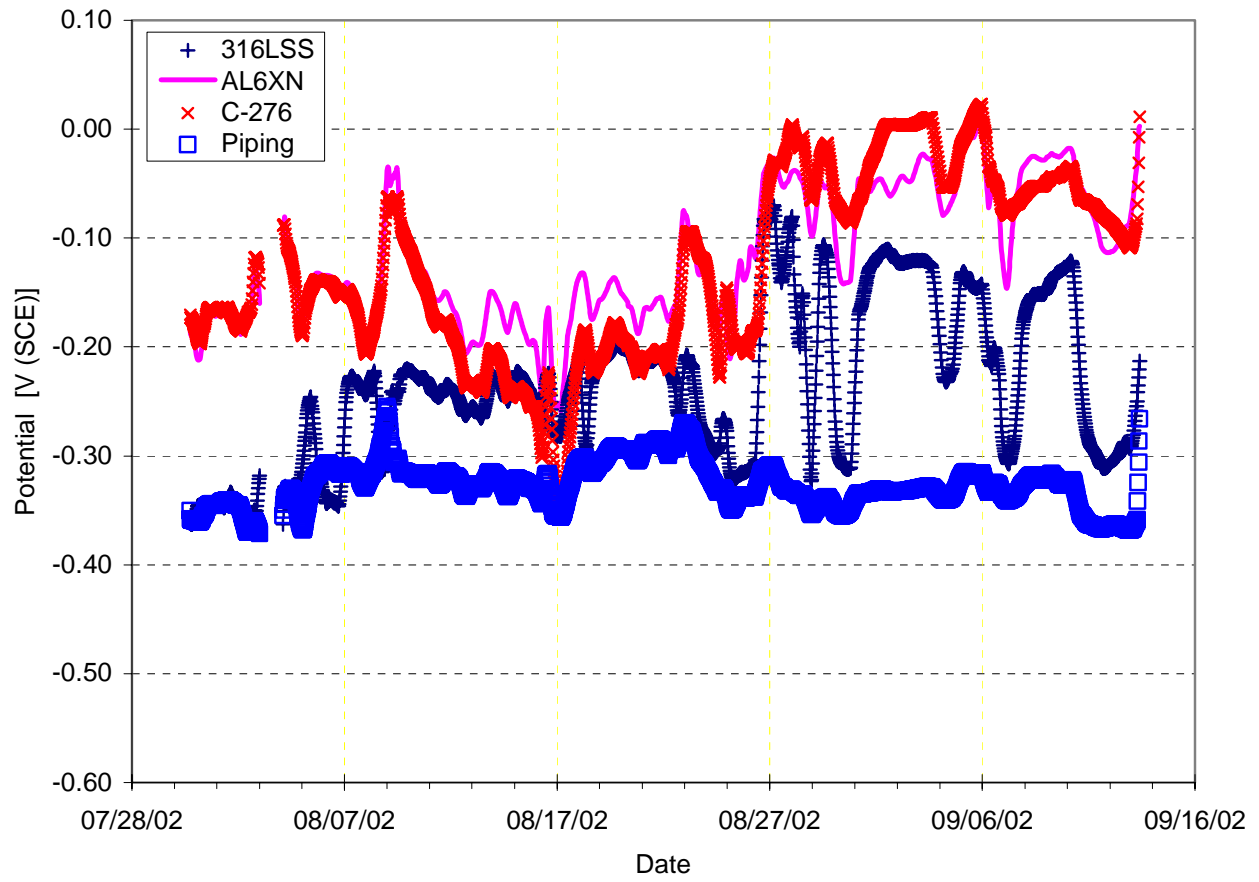


FIGURE 8. Electrochemical potentials of the different probes in and the piping system of the side loop during the time as shown in Figure 6.

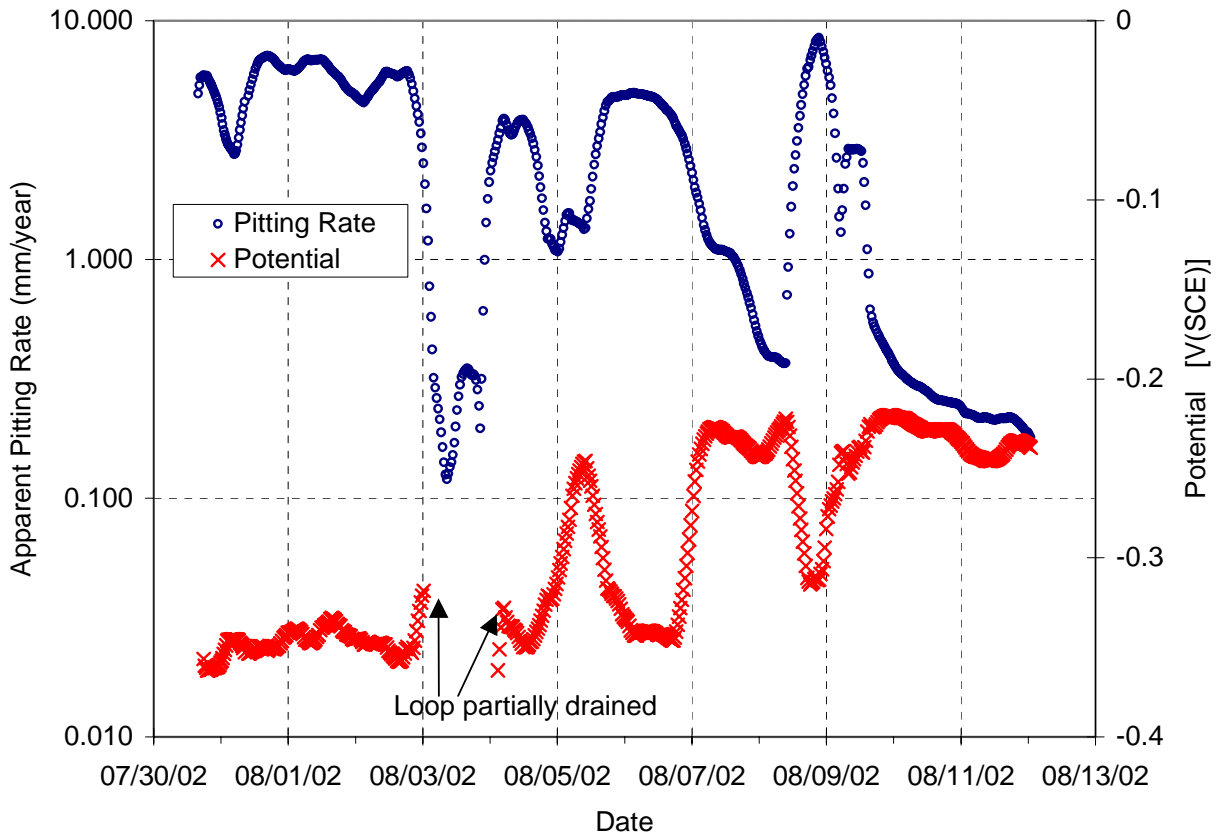


FIGURE 9. Comparison between the apparent pitting rate and potential for the Type 316L stainless steel probe.

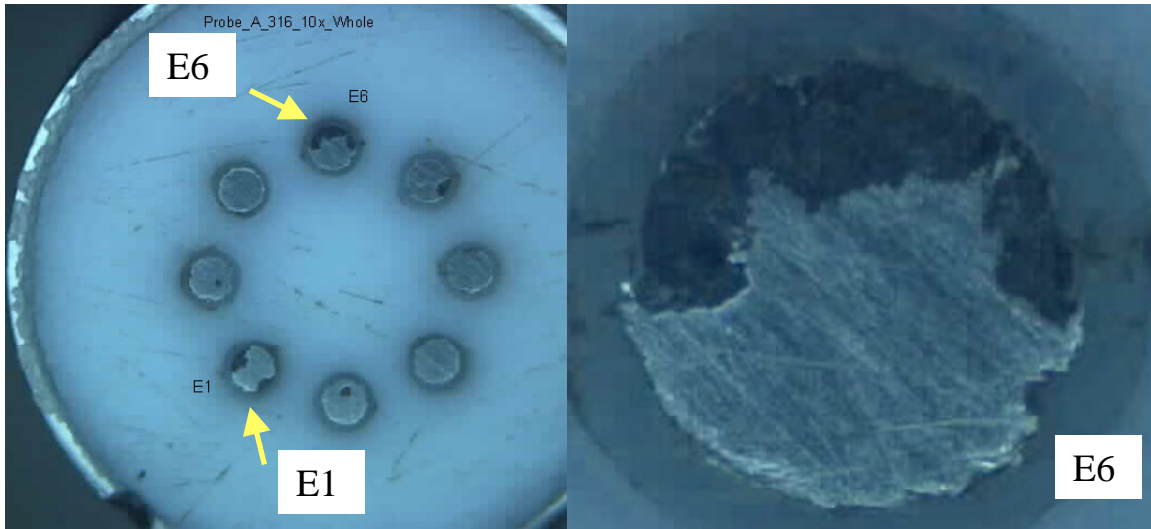


FIGURE 10. The sensing surface of the Type 316L stainless steel probe after 45-day service in the side loop of a hot brine stream. Severe pitting corrosion is apparent on some electrodes.

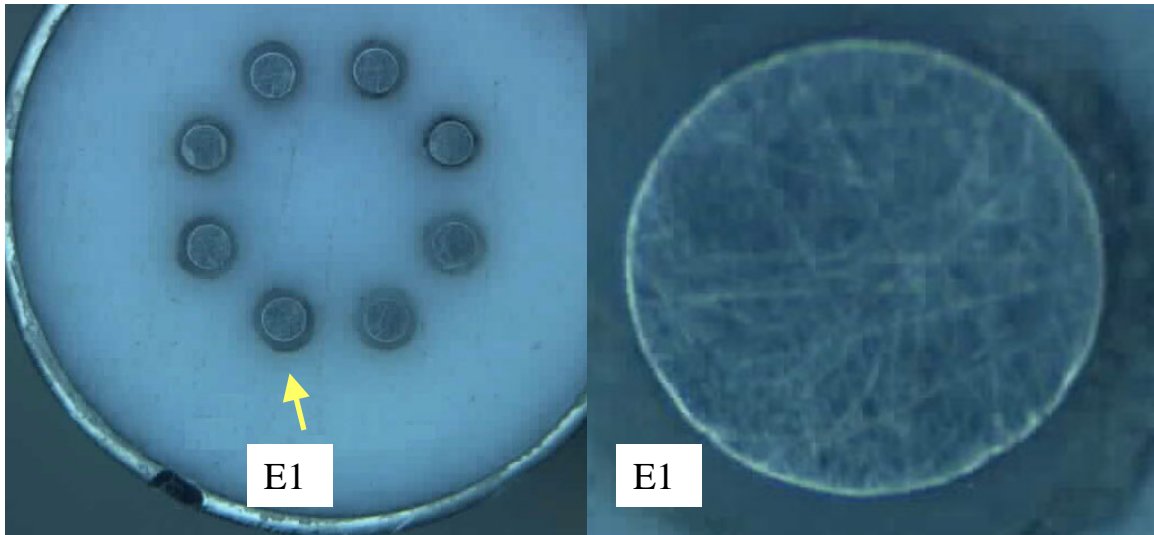


FIGURE 11. The sensing surface of the AL6XN probe after 45-day service in the side loop of a hot brine stream. No apparent pitting corrosion could be visually seen.

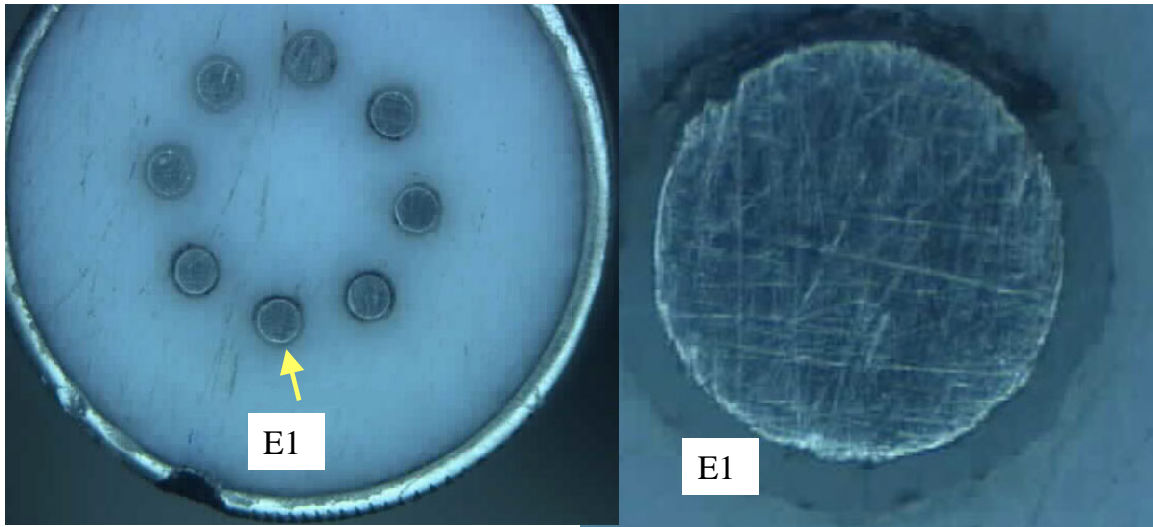


FIGURE 12. The sensing surface of the Alloy C-276 probe after 45-day service in the side loop of a hot brine stream. No apparent pitting corrosion could be visually seen.